International Journal of Applied Pharmaceutics

ISSN- 0975-7058 Vol 12, Issue 4, 2020

Original Article

CATIONIC NANOSTRUCTURED LIPID CARRIERS: OPTIMIZATION OF ZETA POTENTIAL AND EVALUATION

MIRZA SALMAN BAIG[1,2*], AQUIL-UR-RAHIM SIDDIQUI[3]

[1]Y. B. Chavan College of Pharmacy, Dr Babasaheb Ambedkar Marathwada University, Aurangabad, Maharashtra, India, [2]Anjuman-i-Islam's Kalsekar Technical Campus, School of Pharmacy, Affiliated to University of Mumbai, Maharashtra, India, [3]Shri Bhagwan College of Pharmacy, Dr Babasaheb Ambedkar Marathwada University, Aurangabad, Maharashtra, India
Email: mirzasalman.pharma@gmail.com

Received: 20 Mar 2020, Revised and Accepted: 15 Apr 2020

ABSTRACT

Objective: To fabricate, optimize and evaluate, Lipid-based cationic nanoparticulate dispersed system to improve the bio-adhesion property for ophthalmic use.

Methods: Lipid-based cationic nanoparticulate dispersed system was fabricated by melt emulsification ultrasonication method and Box-Behnken design was utilized for optimization of formulation through the Design-Expert® program. The concentration of stabilizer, liquid lipid and Cetyltrimethylammonium Bromide (CTAB) was selected as variables (factors) while particle size, zeta potential and polydispersity index (PDI) were selected as a response for optimization purpose. Characterization of particle properties was performed using Transmission Electron Microscopy (TEM), Photon correlation spectroscopy (PCS). Fourier-transform infrared spectroscopy (FT-IR) was performed to study chemical interaction among ingredients. Rhodamine B entrapped CNLC formulation was used to study the interaction of NLC and CNLC on a three-dimensional and two-dimensional ocular tissue model for cell uptake and penetration properties.

Results: Cationic nanostructured lipid carrier system was successfully fabricated by melt emulsification ultrasonication method. Characterization of nanoparticulate system using PCS revealed particle size in the range of 113.1 to 274.2 nm, PDI in a range of 0.147 to 0.280, while zeta potential in the range of 7.2 to 49.8 mV. The validation of statistical design suggested that it was suitable for navigation of design space. TEM imaging confirmed the results of PCS characterization. FT-IR study suggested a minimal chemical interaction among ingredients in CNLC. Confocal laser microscopic imaging for the interaction of NLC and CNLC on a three-dimensional and two-dimensional ocular tissue model revealed good penetration and bio-adhesion properties.

Conclusion: The fabricated Cationic nanostructured lipid carrier system was found to be the potential ophthalmic novel drug delivery system with good bio-adhesion and penetration properties.

Keywords: SLN, NLC, CNLC, Cationic Nanostructured Lipid Carriers, Design-Expert, Ocular, Ophthalmic, Drug delivery, Nanoparticles, Cell uptake

DOI: http://dx.doi.org/10.22159/ijap.2020v12i4.37531. Journal homepage: https://innovareacademics.in/journals/index.php/ijap

INTRODUCTION

Topical instillation of the eye drops is a popular method for ophthalmic medicines. But this method suffers many challenges because of anatomy and physiology of eye. Physiological factors like the blinking of eyes and tear turn over results in spillage of medicine [1]. Also, there are other barriers like cornea, which limit the permeation of the medicine [2]. The volume of the cul-de-sac is very less hence a large volume of medicines can't be instilled. Frequent instillation of the drug is a tedious task with low patient compliance [3]. All these reasons result in the poor therapeutic efficacy of topically administered ophthalmic medicine. Hence, there was a need of novel ophthalmic drug carrier system which could improve the efficacy of medicine through topical rout [4-6]

Nanostructured lipid carrier (NLC) are lipid-based nanoparticulate system prepared by adding liquid lipids along with solid lipid [7]. These colloidal lipid carriers are bio-degradable and show good entrapment efficiency compare to solid lipid nanoparticles (SLN). Cationic nanostructured lipid carrier (CNLC) are functional nanostructured lipid carriers which possesses positive charge on its surface [8]. Positive charge on its surface provide good adherence property to body cells while liquid lipid is incorporated to enhance drug loading capacity of lipid carrier [9]. Small size of particles in the nanometric range could make it permeable to the desired site for action. These properties of CNLC makes it a suitable candidate as the novel colloidal carrier for targeted drug delivery, especially to ocular tissue [10].

The purpose of the current study was to know the effect of various ingredients of CNLC like the concentration of stabilizer, liquid lipid, surfactant, type of liquid lipid on particle properties like particle size, zeta potential and polydispersity index (PDI). Different types of liquid lipids were explored like Imwitor, Miglyol and Labrafac to study its effect on properties of nanostructured lipid carriers. The CNLC formulation was prepared using the melt-emulsification ultrasonication method. The CNLC containing the labrafac were further exploited and investigated to develop optimum CNLC formulation. Cetyltrimethylammonium Bromide (CTAB) was added to induce a positive charge on nanoparticles [11].

MATERIALS AND METHODS

Materials

Labrafac PG, Gelucire 50/13 and Compritol 888 atomized, were provided by Gattefossé. Miglyol® 812 N and Imwitor® 948 were a kind gift from IOI Oleo GmbH, Germany. Cetyltrimethylammonium Bromide (CTAB), Hoechst stain solution and Rhodamine B octadecyl ester perchlorate were procured through Sigma-Aldrich. While other reagents were of the analytical grade.

Methods

Preparation of NLC and CNLC

Nanostructured lipid carriers (NLC) and cationic nanostructured lipid carriers (CNLC) were prepared using the melt-emulsification ultrasonic homogenization method as shown in fig. 1 [12, 13]. Stabilizer, Solid lipid and Liquid Lipid were heated in glass vial then Rhodamine B stain was added to molten lipid mix (80 °C), finally pre-heated distilled water was added to molten lipid phase which was then homogenized using a vortex mixer. This coarse dispersion was subjected to probe ultra-sonication and allowed to cool at room temperature to obtain colloid.

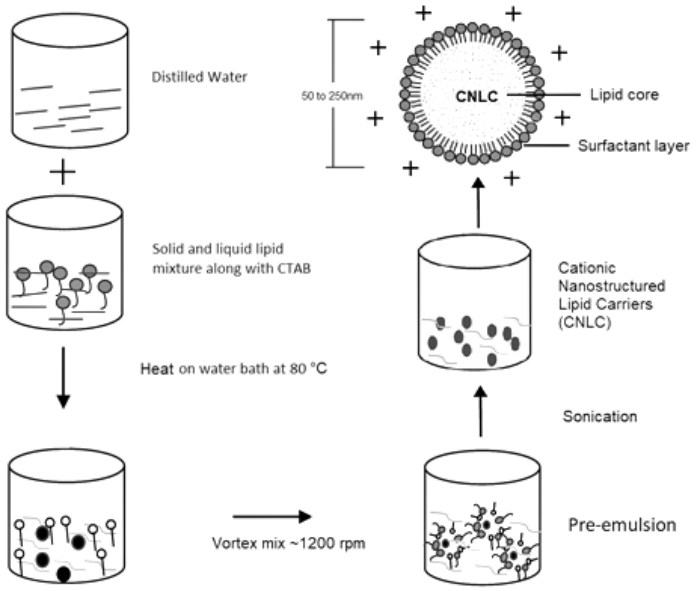

Fig. 1: Method of preparation for CNLC

Photon correlation spectroscopy (PCS)

All the sample were diluted 500 times before measurement. Malvern zeta sizer was employed for Photon correlation spectroscopy [14, 15]. All the readings were noted at 25 °C.

Entrapment of rhodamine-B

Ultracentrifuge filtration method was used for determining percent entrapment efficiency. Centrifugation was done at 3000 G for 20 min. Rhodamine B loaded NLC/CNLC was filtered through 10K molecular weight cut off ultrafilter. The filtrate was analysed using UV absorbance technique for any traces of Rhodamine-B [16].

Transmission electron microscopy (TEM)

Distilled water was added to the sample dilute it up to 100 times, then spreading was done over the copper grid. Sample was air-dried for one hour before imaging. The instrument JEM-1230 JEOL, Japan was used for TEM imaging. The method was used to confirm the shape and size of CNLC formulation [6, 8]

FT-IR spectroscopy

Infra-red spectral analysis of CNLC and physical mixture were performed using Nicolet iS50, Thermo-Fisher FT-IR spectrometer. CNLC formulation or physical mixture was mixed with acetone then spread on calcium fluoride disc. After evaporation of acetone, a thin film so obtained was used to obtain FT-IR [17]. The spectra were collected and processed through OMNIC software.

Tissue culture study

Method of preparation of tissue model

Porcine eyes conjunctival membrane was removed and digested by enzyme collagenase and dispase. The cell culture was prepared in Dulbecco's modified eagle's medium containing glucose along with 5 percent carbon-di-oxide at 37 °C. Also, one percent L-glutamine, ten percent foetal bovine serum, along with one percent antibiotics combination of streptomycin and penicillin was added. The 3D conjunctival tissue model was developed using collagen hydrogels (Fisher Scientific, UK) by incorporating fibroblast cells in it at a density of 80,000 cells/100 µl gel. The supplementary culture medium was added during the preparation of the gel-cell model [18, 19].

Internalization of NLC and CNLC in tissue culture models

To study the effect of rhodamine B loaded NLC-B (without CTAB) and optimum CNLC (with CTAB) formulations on cell internalization capacity, the fibroblast cells were cultured by the above-mentioned method. Cells were incubated with Hoechst reagent for 15 min to stain nuclei with blue colour, then fibroblast cells were incubated separately with 5 percent NLC and 5 percent CNLC formulations into the culture medium for 30 min. The formulation containing culture medium was removed and fresh culture medium was added before cell imaging using a confocal microscope (Olympus) [10, 19]

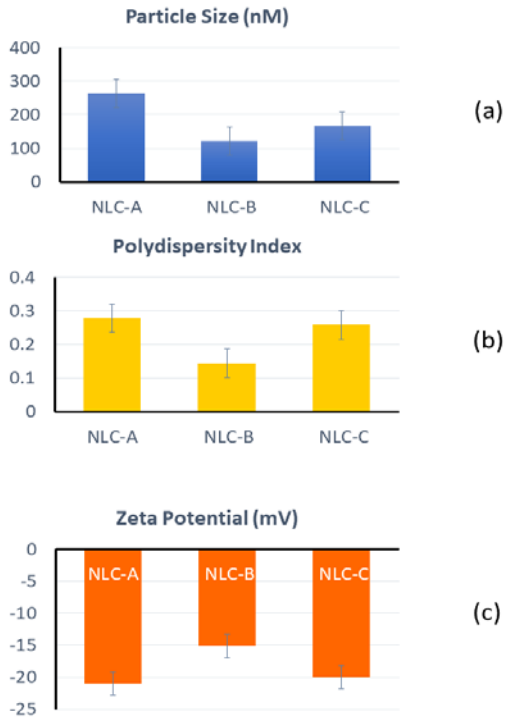

Fig. 2: Graph showing particle-size (a) polydispersity-index (b) and zeta-potential (c) for various NLC formulations (n=3)

Permeation of CNLC in three-dimensional tissue-model

Collagen-based gel was prepared. The fibroblast cells incubated in gel after incubation for around 2 d until the cells elongate. Ten

percent of 'rhodamine B loaded optimum CNLC' prepared in the culture medium. This was added over the gel-based model after removing old culture medium, then incubated for an hour, media before imaging. 3D imaging was done by laser confocal-microscope to study penetration of CNLC across the gel-cell model [13, 19, 20]

RESULTS AND DISCUSSION

Effect of various liquid lipid on properties of NLC

The NLC contain liquid lipid, unlike the Solid Lipid Nanoparticles (SLN). There are profound effects of liquid-lipid on properties of nanoparticles, especially particle size, PDI and entrapment efficiency [6, 14, 21]. The effect of different liquid lipids like Miglyol, Labrafac and Imwitor have been studied for mentioned properties of NLC and CNLC formulations. The decrease in particle size and PDI was observed after the addition of liquid lipid because it caused the lowering of consistency of molten lipid mixture during formulation processes. Low consistency of lipid phase provides more time to internal phase globules to acquire uniform spherical shape before it solidifies; hence a low PDI was observed. Particle size and PDI for Labrafac containing NLC-B was found to be least (fig. 2 a-b) among other NLC formulations containing miglyol and imwitor. While zeta potential for NLC-B was found to be highest among other types of NLC formulations, which are attributed to the miscibility of labrafac with solid lipid (compritol).

Effect of CTAB concentration on properties of CNLC

When the concentration of CTAB was varied from 2.5 to 7.5 mg/ml in CNLC, an increment in zeta potential was observed from 42 to 46.4 mV as shown in fig. 3. CTAB is a cationic surfactant which makes the surface of nanoparticles positively charged [10, 22]. Also, a slight increase in particle-size was observed on the increment of CTAB concentration, probably because of the adsorption of CTAB at the interphase of the solid (nanoparticles) and liquid medium.

Table 1: Formulae for various NLC and CNLC formulations

	Formulation					
Ingredients(per ml)	**NLC-A**	**NLC-B**	**NLC-C**	**CNLC (2.5)**	**CNLC(5)**	**CNLC (7.5)**
Compritol 888 ATO(mg)	20	20	20	20	20	20
Gelucire 50/13(mg)	30	30	30	30	30	30
Miglyol® 812 N(µl)	10	--	--	--	--	--
Labrafac PG ®(µl)	--	10	--	10	10	10
Imwitor® 948(µl)	--	--	10	--	--	--
CTAB(mg)	--	--	--	2.5	5.0	7.5

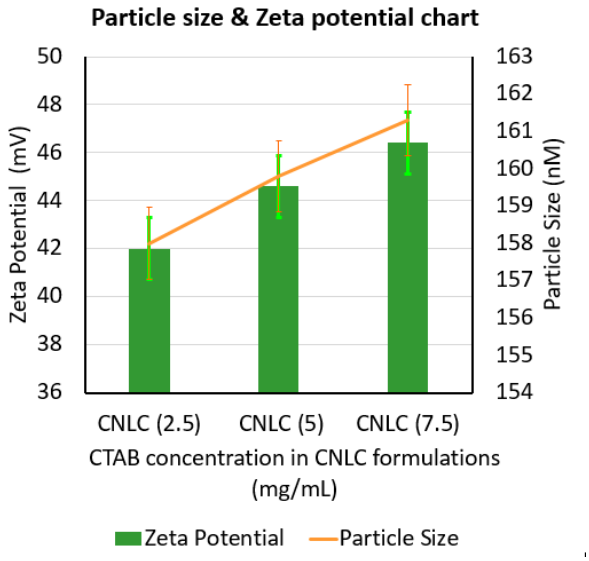

Fig. 3: Graph showing particle size and zeta potential of various CNLC formulations (n=3)

Table 2: Factors and responses for box-behnken experimental design and optimization

	Name	Unit	Factor level in actual		
			Low	**Medium**	**High**
Factor					
X_1	Gelucire	mg/ml	10	20	30
X_2	Labrafac	µl/ml	10	15	20
X_3	CTAB	mg/ml	0.5	2.75	5
Response			**Constraints**		
Y_1	Particle size	nm	Reduce		
Y_2	Polydispersity Index (PDI)		Reduce		
Y_3	Zeta Potential	mV	Augment		

Optimization of CNLC

It was found through studies that concentration of CTAB up to 5 mg/ml was enough to induce positive zeta potential up to 44.6 mV. Hence, a range of CTAB was selected from 0.5 to 5 mg/ml in the CNLC formulation. Optimization constraints for various independent variables are mentioned in table 1.

Design-Expert® software was utilized for optimization studies [13, 23]. The significant factors identified for optimization were concentration of

stabilizer, liquid lipid and CTAB. However, responses observed were particle size, zeta potential and PDI. Total 17 formulation runs were prepared based on the combination of significant independent variables as provided by software and mentioned in table 2. The Box Behnken statistical method was employed for experimental design, because a few numbers of formulation were required for optimization. Experimental values for responses were fed in software for calculation and analysis table 3. The equations which were extracted from software in terms of actual factors could be utilized for making predictions of response for different levels of each factor.

Table 3: Combination of independent variables for experimental design and corresponding responses observed after evaluation of formulations

Formulation no.	Run no.	Independent variables (Factors)			Dependent variables (Response)					
					Actual values			Predicted values		
		Stabilizer (gelucire 50/13) (mg/ml)	Liquid lipid (labrafac) (µl/ml)	CTAB (mg/ml)	Particle size (nm)	PDI	Zeta potential (mV)	Particle size (nm)	PDI	Zeta potential (mV)
		X_1	X_2	X_3	Y_1	Y_2	Y_3	Y_1	Y_2	Y_3
1	12	10	10	2.75	165.6	0.263	38.9	193.26	0.278272	38.20
2	11	30	10	2.75	159.4	0.28	19.5	178.46	0.247022	20.92
3	17	10	20	2.75	274.2	0.147	34.5	297.23	0.180272	33.82
4	10	30	20	2.75	113.1	0.164	13.4	127.53	0.149022	16.55
5	9	10	15	0.5	237.7	0.238	14.6	229.26	0.219647	21.26
6	15	30	15	0.5	129.8	0.165	7.2	129.96	0.188397	3.98
7	6	10	15	5	262.5	0.271	49.8	261.23	0.238897	50.76
8	5	30	15	5	168.7	0.185	28.6	176.03	0.207647	33.48
9	13	20	10	0.5	152.3	0.25	9.1	155.99	0.253022	14.81
10	7	20	20	0.5	194.9	0.178	9.3	203.22	0.155022	10.43
11	8	20	10	5	219.2	0.27	43.5	215.72	0.272272	44.31
12	1	20	20	5	220.4	0.182	36.3	221.54	0.174272	39.93
13	14	20	15	2.75	237.4	0.196	39.6	199.12	0.213647	27.37
14	4	20	15	2.75	193.4	0.208	27.7	199.12	0.213647	27.37
15	3	20	15	2.75	217.6	0.22	31.4	199.12	0.213647	27.37
16	2	20	15	2.75	197.2	0.211	30.2	199.12	0.213647	27.37
17	16	20	15	2.75	241.6	0.204	31.7	199.12	0.213647	27.37

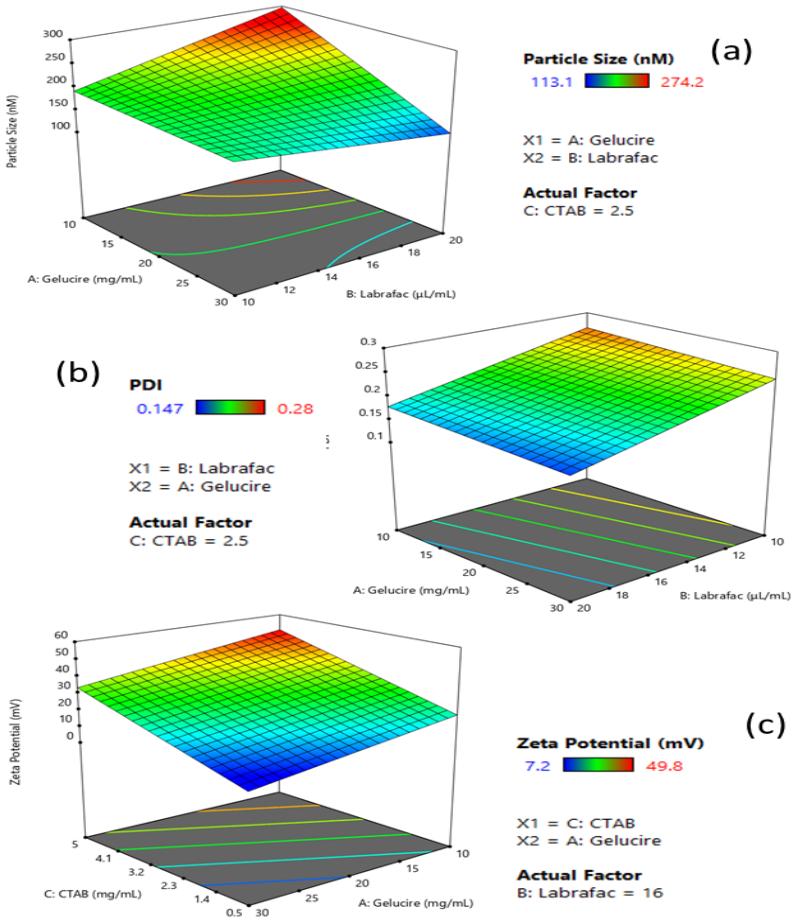

Fig. 4: Three-dimensional response surface graph showing the effect of significant independent variables on particle-size (a), polydispersity-index (b) and zeta-potential (c) of CNLC formulations

Particle size (Y_1)

Size of nanoparticles range from 113.1 to 274.2 nm. The effect of stabilizer (gelucire) and liquid lipid (labrafac) concentration was found to be significant as revealed in fig. 4a. Following equation concerning actual factors represent an effect on particle size.

$$Y_1 = -33.951 + 6.574\,X_1 + 20.672\,X_2 + 19.339\,X_3 - 0.775\,X_1X_2 + 0.157\,X_1X_3 - 0.920\,X_2X_3$$

PDI (Y_2)

Polydispersity index (PDI) range from 0.147 to 0.280. The effect of stabilizer (gelucire) and liquid lipid (labrafac) was found to be significant as revealed in fig. 4b. Increase in liquid lipid concentration reduces PDI. Following equation concerning actual factors represent an effect on PDI.

$$Y_2 = 0.3548 - 0.0011\,X_1 - 0089\,X_2 + 0043\,X_3$$

Zeta potential (Y_3)

Zeta potential range from 7.2 to 49.8 mV. The effect of stabilizer (gelucire) and CTAB was found to be significant as revealed in fig. 4c. Increase in CTAB concentration increases zeta potential. Following equation concerning actual factors represent an effect on zeta potential.

$$Y_3 = 33.1803 - 0.8638\,X_1 - 4375\,X_2 + 6.5555\,X_3$$

Experimental design validation of the model showed good results. Experimental values of dependent variables for those formulations were fed in software for processing. Table 4 shows the report of the model fit summary for Box-Behnken statistical experimental design. The best fit statistical model for particle size was two-factor interaction (2FI) and the best fit statistical model for PDI and zeta potential was linear, while for all the factors, the focus was on the model, maximizing the adjusted R^2 and the predicted R^2.

Fig. 5 revealed the scatter plot for experimental response values plotted against predicted values for dependent variables. Values of adjusted R^2 and predicted R^2 was close enough so that a difference of not more than 0.2 was observed for all the three dependent variables. The run and sequence residual graphs are scatter plot in which externally studentized residuals were plotted against the run number. This represents the randomized run order concerning the time of making formulation, as revealed in fig. 6. Validation of statistical model because of the mentioned reasons make it fit to navigate the design-space of dependent variables.

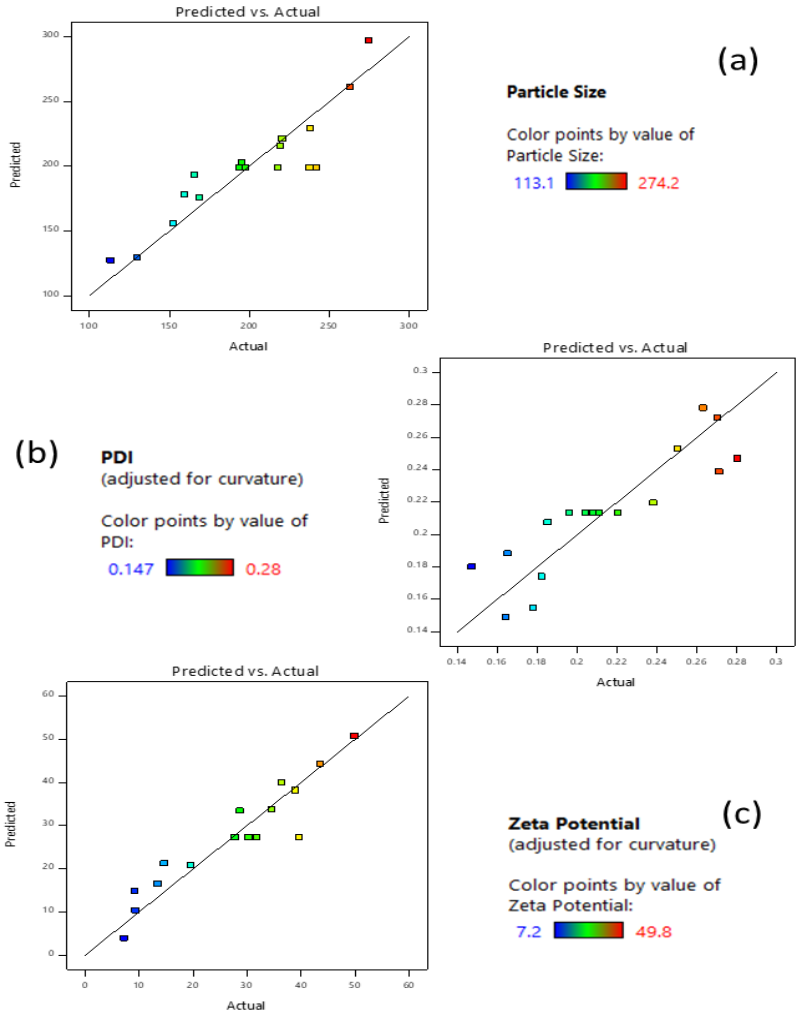

Fig. 5: Graph showing predicted vs actual values for particle-size (a), polydispersity-index (b) and zeta-potential (c)

FT-IR spectroscopy

Infrared spectrometry is a tool to study the interaction among the ingredients of nanoparticles [17]. Fig. 7 revealed FT-IR of optimum CNLC and physical mixture of all its ingredients in a similar proportion. A strong peak was observed at 3100 cm^{-1} in both the spectra because of the hydroxyl-OH stretching. Also, a peak near 1650 cm^{-1} in both the spectra was observed because of C=O functional group stretching. FT-IR study suggest the chemical stability of ingredients in CNLC with minimal interaction.

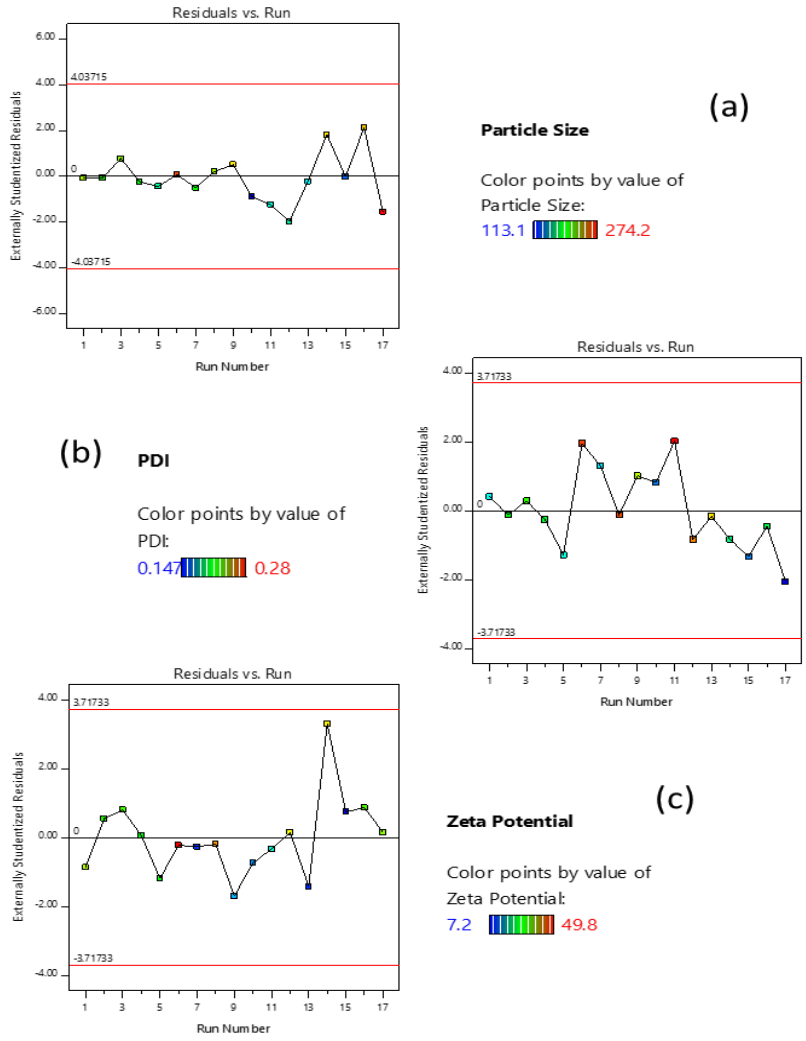

Fig. 6: Scatter plot showing run sequence vs externally studentized residual for particle-size (a) polydispersity-index (b) and zeta-potential (c)

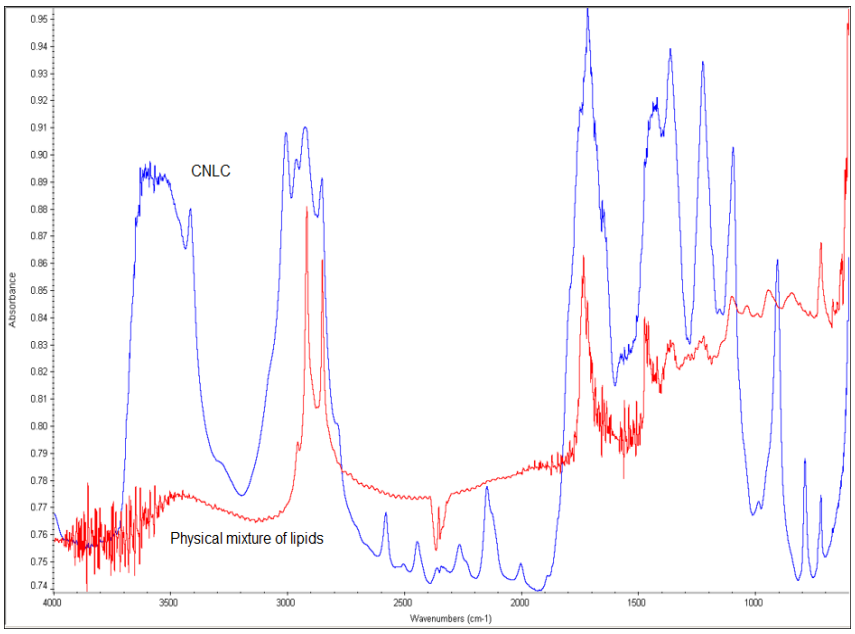

Fig. 7: FT-IR graph for optimum CNLC formulation and physical mixture of its ingredients

Entrapment of rhodamine-B

10 µg/ml of rhodamine was added to the lipid phase of NLC/CNLC during its preparation. A 100 % of entrapment was observed as no trace of rhodamine was observed in the filtrate, when filtered by ultracentrifuge filtration technique.

Transmission electron microscopy (TEM)

Transmission electron microscopy was performed to investigate particulate morphology. TEM image of optimum CNLC in fig. 8 revealed spherical shape particles with small particle size (~ 200 nm). Results of particle size found to agree with results of hydrodynamic diameter of nanoparticles, investigated by PCS technique. Turbid background was because of molecular level dispersion of gelucire in the medium.

Cellular uptake

Comparison rhodamine loaded nanoparticles formulation with CTAB (optimum CNLC) and without CTAB (NLC) was done to study its effect on cell uptake. Confocal laser microscopy used to study the threshold of nanoparticles uptake for both the formulations. Fig. 9a and 9b revealed that there was a profound difference in internalization with high uptake for CLNC while low cell uptake for NLC. High cellular uptake of optimum CNLC was attributed to bio-adhesion of positively charged nanoparticles to negatively charged cell membrane because of electrostatic attraction [10]. Fig. 9c shows permeation of rhodamine entrapped CNLC by microscopic focus stacking through a three-dimensional conjunctival tissue model, which was prepared using collagen. A good permeation of the optimized CNLC was observed through the ocular tissue model.

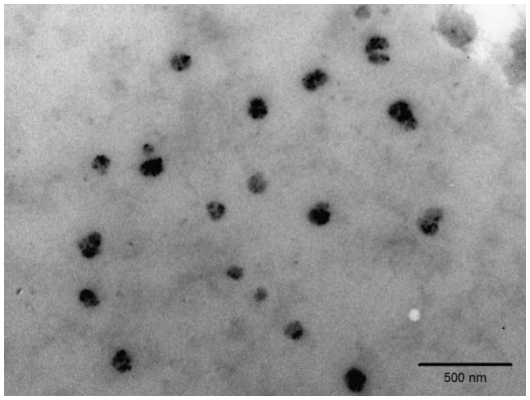

Fig. 8: Transmission electron microscopy (TEM) image for rhodamine optimum CNLC formulation

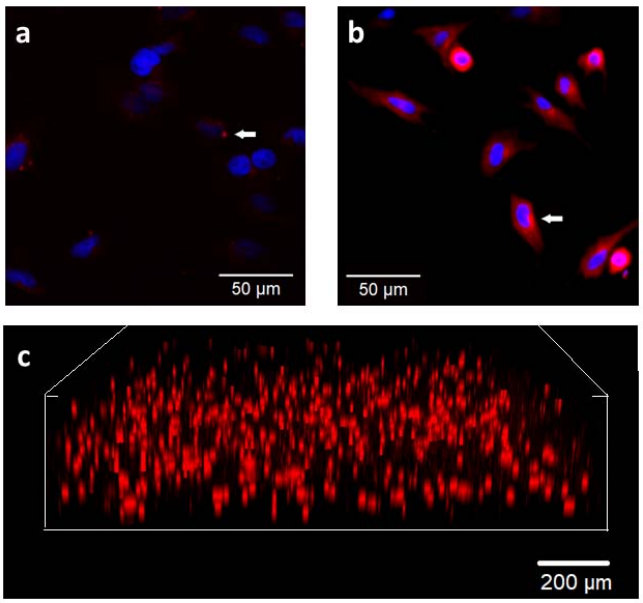

Fig. 9: Image showing, cellular uptake (indicated with white arrow) of rhodamine loaded NLC-B formulation by conjunctival fibroblast 2D cell model (a), cellular uptake of rhodamine loaded optimum CNLC formulation by fibroblast 2D cell model (b) and an image showing 3D collagen gel permeation of rhodamine loaded optimum CNLC formulation (c)

CONCLUSION

A lipid-based colloidal nanoparticulate system CNLC was developed and compared with NLC for its cell interaction property. CNLC was found to be a better carrier system because it showed high cell uptake. The CNLC possesses of positive charge on its surface; hence it provides bio adhesion to the negatively charged membrane of conjunctiva fibroblast cells. Hence, we conclude CNLC holds potential as a novel ophthalmic drug-delivery system for hydrophobic drug molecules.

FUNDING

Nil

AUTHORS CONTRIBUTIONS

Mirza Salman Baig: Research work, data acquisition, conceptualization and writing the original manuscript. Aquil-ur-Rahim Siddiqui: Review manuscript and supervision.

CONFLICT OF INTERESTS

There are not any conflicts of interest

REFERENCES

1. Sanchez Lopez E, Espina M, Doktorovova S, Souto EB, García ML. Lipid nanoparticles (SLN, NLC): Overcoming the anatomical and physiological barriers of the eye–part I–barriers and determining factors in ocular delivery. Eur J Pharm Biopharm 2017;110:70–5.
2. Sanchez Lopez E, Espina M, Doktorovova S, Souto EB, Garcia ML. Lipid nanoparticles (SLN, NLC): overcoming the anatomical and physiological barriers of the eye–part II-ocular drug-loaded lipid nanoparticles. Eur J Pharm Biopharm 2017;110:58–69.
3. Lang JC. Ocular drug delivery conventional ocular formulations. Adv Drug Delivery Rev 1995;16:39-43.
4. Dholakia M, Dave R, Thakkar V, Rana H, Gohel M, Patel N. Newer ophthalmic in situ gel of moxifloxacin hydrochloride:

optimization using box behnken statistical design. Int J Pharm Pharm Sci 2018;10:5.

5. Niamprem P, Srinivas SP, Tiyaboonchai W. Development and characterization of indomethacin-loaded mucoadhesive nanostructured lipid carriers for topical ocular delivery. Int J Appl Pharm 2018;10:91–6.
6. Baig MS, Ahad A, Aslam M, Imam SS, Aqil M, Ali A. Application of box-behnken design for preparation of levofloxacin-loaded stearic acid solid lipid nanoparticles for ocular delivery: optimization, *in vitro* release, ocular tolerance, and antibacterial activity. Int J Biol Macromol 2016;85:258–70.
7. Das S, Ng WK, Tan RBH. Are nanostructured lipid carriers (NLCs) better than solid lipid nanoparticles (SLNs): development, characterizations and comparative evaluations of clotrimazole-loaded SLNs and NLCs? Eur J Pharm Sci 2012;47:139–51.
8. Liu R, Wang S, Sun L, Fang S, Wang J, Huang X, *et al.* A novel cationic nanostructured lipid carrier for improvement of ocular bioavailability: design, optimization, *in vitro* and *in vivo* evaluation. J Drug Delivery Sci Technol 2016;33:28–36.
9. Botto C, Mauro N, Amore E, Martorana E, Giammona G, Bondì ML. Surfactant effect on the physicochemical characteristics of cationic solid lipid nanoparticles. Int J Pharm 2017;516:334–41.
10. Fangueiro JF, Andreani T, Egea MA, Garcia ML, Souto SB, Silva AM, *et al.* Design of cationic lipid nanoparticles for ocular delivery: development, characterization and cytotoxicity. Int J Pharm 2014;461:64–73.
11. Oyewumi MO, Wehrung D, Sadana P. Gelucire-stabilized nanoparticles as a potential DNA delivery system. Pharm Dev Technol 2016;21:647–54.
12. Date AA, Vador N, Jagtap A, Nagarsenker MS. Lipid nanocarriers (GeluPearl) containing amphiphilic lipid gelucire 50/13 as a novel stabilizer: Fabrication, characterization and evaluation for oral drug delivery. Nanotechnology 2011;22:275102.
13. Baig MS, Owida H, Njoroge W, Siddiqui A ur R, Yang Y. Development and evaluation of cationic nanostructured lipid carriers for ophthalmic drug delivery of besifloxacin. J Drug Delivery Sci Technol 2020;55:101496.
14. Aslam M, Aqil M, Ahad A, Najmi AK, Sultana Y, Ali A. Application of Box-Behnken design for preparation of glibenclamide loaded lipid-based nanoparticles: optimization, *in vitro* skin permeation, drug release and *in vivo* pharmacokinetic study. J Mol Liq 2016;219:897–908.
15. Ameeduzzafar, Imam SS, Bukhari SNA, Ali A. Preparation and evaluation of novel chitosan: gelrite ocular system containing besifloxacin for topical treatment of bacterial conjunctivitis: scintigraphy, ocular irritation and retention assessment. Artif Cells Nanomed Biotechnol 2018;46:959–67.
16. Gardouh A, H Faheim S, M Solyman S. Design, optimization and *in vitro* evaluation of antifungal activity of nanostructured lipid carriers of tolnaftate. Int J Pharm Pharm Sci 2019;11:109–15.
17. Kumar S, Bhanjana G, Kumar A, Taneja K, Dilbaghi N, Kim KH. Synthesis and optimization of ceftriaxone-loaded solid lipid nanocarriers. Chem Phys Lipids 2016;200:126–32.
18. Hornof M, Toropainen E, Urtti A. Cell culture models of the ocular barriers. Eur J Pharm Biopharm 2005;60:207–25.
19. Gater R, Ipek T, Sadiq S, Nguyen D, Jones L, El Haj A, *et al.* Investigation of conjunctival fibrosis response using a 3D glaucoma tenon's capsule+conjunctival model. Invest Ophthalmol Vis Sci 2019;60:605–14.
20. Moghddam SMM, Ahad A, Aqil M, Imam SS, Sultana Y. Optimization of nanostructured lipid carriers for topical delivery of nimesulide using box–behnken design approach. Artif Cells Nanomed Biotechnol 2017;45:617–24.
21. Gupta H, Aqil M, Khar RK, Ali A, Bhatnagar A, Mittal G. Sparfloxacin-loaded PLGA nanoparticles for sustained ocular drug delivery. Nanomed Nanotechnol Biol Med 2010;6:324–33.
22. Khan AM, Mehmood A, Sayed M, Nazar MF, Ismail B, Khan RA, *et al.* Influence of acids, bases and surfactants on the photocatalytic degradation of a model dye rhodamine B. J Mol Liq 2017;236:395–403.
23. Patil A, Lakhani P, Taskar P, Wu KW, Sweeney C, Avula B, *et al.* Formulation development, optimization, and *in vitro–in vivo* characterization of natamycin-loaded PEGylated nano-lipid carriers for ocular applications. J Pharm Sci 2018;107:2160-71.